

Dynamics in Organic Ionic Liquids in Distinct Regions Using Charged and Uncharged Orientational Relaxation Probes

Kendall Fruchey and M. D. Fayer*

Department of Chemistry, Stanford University, Stanford, California 94305

Received: November 23, 2009; Revised Manuscript Received: January 6, 2010

The temperature-dependent fluorescence anisotropy decay (orientational relaxation) of perylene and sodium 8-methoxyperylene-1,3,6-sulfonate (MPTS) were measured in a series of 1-alkyl-3-methylimidazolium bis(trifluoromethanesulfonyl)imide (alkyl = ethyl, butyl, hexyl, octyl) organic room temperature ionic liquids (RTIL). The two fluorescent probe molecules display markedly different rotational dynamics when analyzed using Stokes–Einstein–Debye theory, demonstrating that they are located in distinct environments within the RTILs and have very different interactions with their surroundings. Perylene rotates with subslip behavior, becoming increasingly subslip as the length of ionic liquid alkyl chain is increased. The dynamics approach those of perylene in an organic oil. In contrast, MPTS shows superstick behavior, likely reflecting very strong coordination with the RTIL cations. These results are consistent with different elements of rotational friction within the ionic liquid structure, which are available to solutes depending on their chemical functionality.

I. Introduction

As experimental studies on organic room temperature ionic liquids (RTIL) converge on a cogent picture of liquid structure and dynamics, important questions remain regarding the influence of local chemical environments on solute molecules. The interaction of an ionic liquid solvent with dissolved solute is of particular importance to many of the proposed applications such as reaction solvents,^{1–3} separations,⁴ and batteries.⁵ These issues have strong dynamical underpinnings that time dependent studies can address.

A particularly important and distinguishing characteristic of organic ionic liquids is the concept of nanoscale heterogeneity. Originally identified in MD simulations,⁶ the concept has gained considerable traction as a diverse range of experimental studies appear to confirm the existence of structures that persist on non-negligible time scales.^{7–11} These proposed ionic liquid structures contain hydrophobic regions of alkyl “tails,” and charge-ordered, hydrophilic “head group” regions. In the context of this liquid structure, strong elements of selective solvation are possible. The resulting diversity of local environments can have a direct impact on the dynamics of processes where solvation environment is important. The effect of environment has been observed in the context of a photoisomerization.¹² It is not difficult to consider the importance of dynamic heterogeneity being expanded beyond selective excitation in photochemical reactions to include differences in transport properties and availability of reagents and catalysts in the ionic liquid matrix.

One appeal of RTILs as a reaction medium is the breadth of molecules they can solvate. It is not unreasonable to ascribe this to the presence of multiple chemical environments. Dynamic heterogeneity may have a nontrivial impact on the reaction dynamics, and therefore influence “task-specific” organic ionic liquids.¹³ The design of task-specific organic ionic liquids may depend on the dynamics of molecules in distinct environments in addition to the specific substrate interactions.

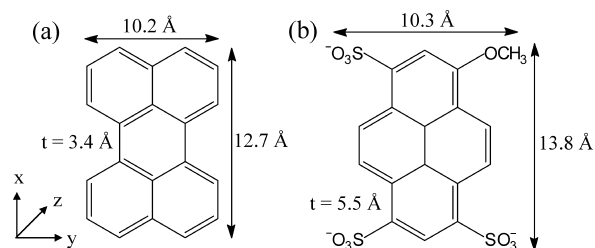


Figure 1. Dimensions and coordinate system for perylene (a) and MPTS (b). The out of plane thickness is labeled t .

In this study, the orientational relaxation dynamics of perylene and sodium 8-methoxyperylene-1,3,6-sulfonate (MPTS) were determined using time dependent fluorescence anisotropy measurements. Perylene and MPTS reflect two extremes of chemical functionalities (see Figure 1). Perylene is neutral and nonpolar. In contrast, MPTS has three negatively charge sulfonate groups. These two probe molecules will likely interact with the separate elements of the charged and nonpolar environments in the ionic liquid structure. The series of ionic liquids of alkyl-substituted imidazolium bis(trifluoromethanesulfonyl)imide (abbreviated as $C_n\text{mim}^+ \text{NTf}_2^-$) was chosen as a class of relatively hydrophobic ionic liquids that can be obtained at high purities. They have fairly low viscosities and should demonstrate prototypical ionic liquid behavior. Furthermore, for imidazolium cations, there have been indications that a minimum chain length is required for formation of nanostructure environments.⁶

For each liquid, the orientational relaxation and the viscosity were measured as a function of temperature. These measurements permit the details of the probe interactions with its environment to be explicated. The results demonstrate that perylene and MPTS are located in distinct environments and experience very different interactions with their surrounding. Perylene rotates with subslip behavior, becoming increasingly subslip as the length of RTIL alkyl chain is increased. In contrast, MPTS shows superstick behavior, likely reflecting very strong coordination with the RTIL cations. These results are consistent with different elements of rotational friction within

* To whom correspondence should be addressed. E-mail: fayer@stanford.edu.

the ionic liquid local structures that are available to solutes depending on their chemical functionality.

Previous fluorescence studies of orientational relaxation of RTILs have seen Debye–Stokes–Einstein (DSE) behavior¹⁴ and possibly deviations from DSE behavior.^{15–17} Most of the studies examined very polar and charged dye molecules. Mali et al. studied a charged dye molecule and a nonpolar chromophore in a single RTIL.¹⁵ The studies presented here examine a triply charged fluorophore and a neutral nonpolar fluorophore that are similar in size (see Figure 1) in a series of RTILs with increasing hydrocarbon chain lengths. The temperature dependent studies of the orientational relaxation permit the local friction to be extracted from the data. By measuring the orientational relaxation on the series of liquids, it is possible to examine changes in the nature of the local environments experienced by the two types of probe molecules.

II. Experimental Procedures

All ionic liquids were purchased from IoLiTec at 99+% HP grade. The fluorophores were purchased from Aldrich and used without further purification. HPLC grade water (Fisher) and DMSO (Mallinckrodt AR grade) were distilled prior to use. Light paraffin oil (Fisher) was used without modification. The ionic liquids were dried upon receipt under vacuum at 60 °C for 1 day, and then transferred into a nitrogen glovebox for storage and sample preparation. Water content was measured for all ionic liquid samples using Karl Fischer titration (Mettler DL39) and is less than 75 ppm water by weight. The optical samples were prepared from stock solutions by dissolving the chromophore at a standardized concentration in a volatile solvent (hexane for perylene and methanol for MPTS). A 1 cm quartz cuvette was filled with an appropriate amount of stock solution and then the solvent evaporated under gentle heat and dry nitrogen. These were transferred into the glovebox and stirred with aliquots of the ionic liquid to a 0.3 optical density, corresponding to a chromophore concentration of approximately 8×10^{-6} M for both dyes. One consequence of note resulting from the sample preparation technique is the absence of dissolved O₂ in any of the ionic liquid samples. Nonionic liquid solvents were purged with nitrogen to remove O₂, but the fluorophores showed slightly shorter lifetimes owing to the incomplete removal of oxygen.

The measurements were made with time correlated single photon counting (TCSPC), and the experimental setup is described elsewhere.¹⁸ The samples were housed in a computer controlled cryostat (Janis ST-100) stable to ± 0.1 K. The instrument response was measured to be 40 ps using a scattering sample. Time dependent fluorescence data were collected at each temperature (298 to 333 K in 5 K increments) in parallel, perpendicular, and magic angle (54.7°) polarizer orientations. Samples were excited at 380 nm for MPTS and 409 nm for perylene. The excitation pulses were single pulses selected at 4 MHz rate from a Ti:Sapphire oscillator and doubled to the excitation wavelengths. Fluorescence, after passing through an appropriate long pass filter to remove excitation light, was observed at 420 nm for MPTS and 469 nm for perylene with a channel plate detector on a monochromator.

Steady-state fluorescence spectra were collected at room temperature using a Fluorolog-3 fluorimeter. Fluorescence spectra were collected in the forward-facing geometry with excitation at 380 nm with correction for lamp fluctuation and monochromator/detector efficiency. Temperature dependent viscosities of paraffin oil were measured using a Cannon-Ubbelohde viscometer in a constant temperature bath. Other

viscosities were taken from the literature.¹⁹ Since RTIL viscosity can be dramatically affected by small impurity concentrations, the room temperature viscosities were confirmed in a nitrogen purged environment using a Texas Instruments AR-G2 rheometer with 40 mm parallel plate geometry.

III. Results and Discussion

The fluorescence experiments measure the time dependent anisotropy, $r(t)$, defined as

$$r(t) = \frac{I_{\parallel}(t) - I_{\perp}(t)}{I_{\parallel}(t) + 2I_{\perp}(t)} \quad (1)$$

with I_{\parallel} and I_{\perp} the time dependent fluorescence intensities polarized parallel and perpendicular to the excitation beam, respectively. Eisenthal and Chung presented the functional form of the fluorescence anisotropy decay for the most general case of orientational diffusion.²⁰ The result is a sum of 5 exponentially decaying terms containing rotational diffusion constants D_j about the j th molecular axis as

$$r(t) = \frac{6}{5}(q_y q_z \gamma_y \gamma_z e^{-3(D_x+D)t} + q_x q_z \gamma_x \gamma_z e^{-3(D_y+D)t} + q_x q_y \gamma_x \gamma_y e^{-3(D_z+D)t}) + \frac{3}{10}(\beta + \alpha)e^{-(6D+2\Delta)t} + \frac{3}{10}(\beta - \alpha)e^{-(6D-2\Delta)t} \quad (2)$$

for

$$\alpha = \frac{1}{\Delta}[D_x(q_y^2 \gamma_y^2 + q_z^2 \gamma_z^2 - 2q_x^2 \gamma_x^2 + q_x^2 + \gamma_x^2) + D_y(q_x^2 \gamma_x^2 + q_z^2 \gamma_z^2 - 2q_y^2 \gamma_y^2 + q_y^2 + \gamma_y^2) + D_z(q_x^2 \gamma_x^2 + q_y^2 \gamma_y^2 - 2q_z^2 \gamma_z^2 + q_z^2 + \gamma_z^2) - 2D]$$

$$\beta = q_x^2 \gamma_x^2 + q_y^2 \gamma_y^2 + q_z^2 \gamma_z^2 - \frac{1}{3}$$

$$D = \frac{1}{3}(D_x + D_y + D_z)$$

$$\Delta = \sqrt{(D_x^2 + D_y^2 + D_z^2 - D_x D_y - D_x D_z - D_y D_z)}$$

The quantities q_j and γ_j are projections of the excitation and emission dipole onto the molecular axes. For most rotators, the similarity of the rotational diffusion constants generally causes there to be fewer than 5 resolvable exponentials, oftentimes generating only a single rotational diffusion constant.

In the experiments presented here, the observed exponential decays were related to hydrodynamic properties through the Debye–Stokes–Einstein relation

$$\tau = \frac{1}{6D} = \frac{\eta V f C}{kT} \quad (3)$$

where τ is the measured orientational relaxation time constant, η the viscosity, k is the Boltzmann constant, V is the molecular volume, C is a friction coefficient, and f is the shape factor.

TABLE 1: Shape Factors and Slip Friction Coefficients

	shape factors				slip coefficients			
	f_x	f_y	f_z	f	C_x	C_y	C_z	C
perylene	1.86	1.38	2.03	1.76	0.23	0.65	0.015	0.085
MPTS	1.43	1.01	1.55	1.33	0.10	0.54	0.032	0.110

For a given molecule, the friction coefficient will contain information on the rotational friction experienced by the molecule. For large particles, the stick boundary condition ($C = 1$) almost always holds. For rotators of similar size to the solvent molecules, the continuum approximation of the solvent begins to break down. This is manifest as a decrease in friction toward the slip limit, for which the value of C depends on the geometry of the rotator.

Figure 1 shows the structures and dimensions of the fluorophores used in this study. For both molecules, the shape is close to ellipsoidal based on a geometrically minimized structure. Using the van der Waal radii of the constituent atoms, molecular volumes of 225 Å³ for perylene and 343 Å³ MPTS were calculated. From the molecular dimensions, the shape factors²¹ and theoretical slip friction coefficients^{22,23} can also be generated. These quantities are listed in Table 1.

A. Perylene. Because of the high D_{2h} symmetry of perylene, the equation for the fluorescence anisotropy simplifies to

$$r(t) = 0.3(\alpha - \beta)e^{-(6D+2\Delta)t} + 0.3(\alpha + \beta)e^{-(6D-2\Delta)t} \quad (4)$$

Equation 4 can be further simplified if one assumes the behavior of an oblate spheroid rotator, that is $D_x = D_y \ll D_z$, using the coordinate system of Figure 1. Under these conditions, eq 4 can be expressed as

$$r(t) = 0.1e^{-(2D_x+4D_z)t} + 0.3e^{-6D_z t} \quad (5)$$

Anisotropy studies of perylene have often encountered a well-known “anisotropy deficit,” that is, an initial anisotropy of less than the theoretical 0.4.²⁴ While this does not directly impact the information content of the experiment, the prefactors in eq 5 have smaller than the theoretical values of 0.1 and 0.3.

To extract the rotational diffusion constants, measured time dependent anisotropies were fit to a biexponential function convolved with the instrument response using nonlinear least-squares. From the fits, the appropriate diffusion constants can be extracted from linear combinations of the exponential time constants using eq 4. Figure 2 shows the temperature dependent orientational relaxation decay constant, $\tau = 1/6D$, where here D is the average diffusion constant. In all cases except $C_2\text{mim}^+$ ($r^2 = 0.95$), linear regression yields an adjusted correlation coefficient of greater than 0.99, which confirms Debye–Stokes–Einstein behavior.

The results of the analysis are presented in Table 2 as a list of the experimentally determined average friction coefficients (C in eq 3). As the alkyl chain length increases, the friction coefficient approaches that of perylene in paraffin oil. From the values listed in Table 2, perylene is found to rotate with slip boundary conditions.

Because perylene is only slightly larger than the ionic liquid ions, some contribution to the subslip behavior can come from the coarseness of solvent media, which can be treated using Gierer–Wirtz theory. The Gierer–Wirtz theory takes the solvent to be concentric shells of spherical particles around the probe

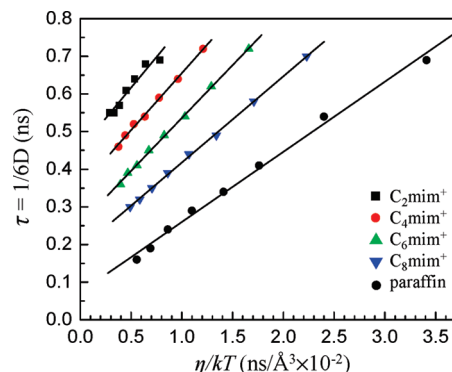


Figure 2. Orientational relaxation times, $\tau = 1/6D$, obtained from the average diffusion coefficients for perylene in five solvents plotted as a function of the viscosity (η) divided by kT (symbols). The lines through the data points are fits using linear least-squares. For clarity, the data sets have been shifted up 0.4 ns for $C_2\text{mim}^+$, 0.3 ns for $C_4\text{mim}^+$, 0.2 ns for $C_6\text{mim}^+$, and 0.1 ns for $C_8\text{mim}^+$.

TABLE 2: Perylene Exp. Frictional Coefficients, C

solvent	friction coefficient
$C_2\text{mim}^+$	0.0858 ± 0.008
$C_4\text{mim}^+$	0.0799 ± 0.002
$C_6\text{mim}^+$	0.0733 ± 0.001
$C_8\text{mim}^+$	0.0583 ± 0.0007
paraffin oil	0.0483 ± 0.001
theory slip	0.085

solute. For a solvent volume V_s smaller than probe solute volume V_p , the theory expresses the friction coefficient as

$$C = \sigma C_0$$

$$\sigma = \frac{1}{1 + 6(V_s/V_p)^{1/3} C_0} \quad (6)$$

$$C_0 = \left[\frac{6(V_s/V_p)^{1/3}}{(1 + 3(V_s/V_p)^{1/3})^4} + \frac{1}{(1 + 4(V_s/V_p)^{1/3})^3} \right]^{-1}$$

A volume of 163 Å³ was used for V_s , which is approximately the value for both the $C_4\text{mim}^+$ and NTf_2^- ions. Using eq 6, a value of $C = 0.18$ for perylene is computed. Because the calculated value is a factor of 2 greater than the measured friction coefficient, and since no reasonable value for V_s can replicate the measurements, the treatment that only considers the sizes of the solvent and solute molecules cannot explain the subslip rotational dynamics of perylene in the RTILs.

Rotational dynamics in the subslip regime have been studied previously^{25,26} and are often attributed to complex solvation structure in the vicinity of the probe molecule. This structuring can lead to effective void spaces through which the molecule can rotate with little hindrance, leading to a decrease in rotational friction below slip. This picture is used to describe the rotational dynamics of tetracene in alcohols.²⁷

In the perylene/RTIL experiments, the degree of subslip increases with increasing alkyl tail length, approaching the value for perylene in paraffin oil at $C_8\text{mim}^+$. Because of the high symmetry of perylene, the biexponential experimental decays permit the rotational diffusion to be further decomposed into components of rotation in-plane (D_z) and out-of-plane (D_x). The results are presented in Table 3 as the ratio of the appropriate

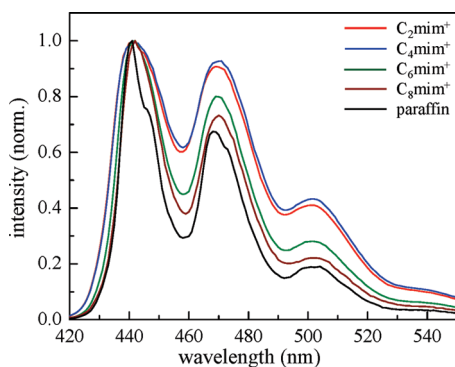
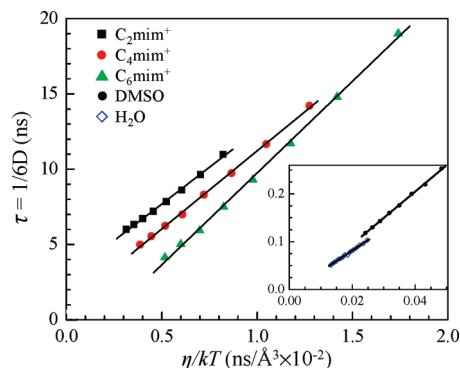
TABLE 3: Ratios of In- and Out-of-Plane Exp. Friction Coefficients to Their Theoretical Slip Values

	in-plane	out of plane
C ₂ mim ⁺	1.2	0.39
C ₄ mim ⁺	1.0	0.44
C ₆ mim ⁺	0.90	0.53
C ₈ mim ⁺	0.67	0.54
paraffin oil	0.55	0.60

friction coefficient to its theoretical value for slip boundary conditions. A value of 1 means that the measured and calculated values are the same. A ratio larger than 1 indicates that the measured value is slower than slip, and a ratio smaller than 1 shows that the experimental value is faster than slip. The trends displayed in Table 3 demonstrate that as the length of the ionic liquid alkyl chain length increases, relative to the theoretical slip values, the in plane rotational diffusion becomes faster with a concurrent slower rotational diffusion out of plane. Both the in-plane and out-of-plane rotational diffusion are converging on the values found in the paraffin oil. The increase of in-plane rotational diffusion constant with alkyl chain length is consistent with previous work on perylene in n-alkanes. For longer alkanes, the results are interpreted as a partial alignment of the alkane chains along the long axis of the perylene.^{28,29} This interpretation is supported by studies of gas phase van der Waal complexes.³⁰ Therefore, the orientational relaxation trends with RTIL chain length indicate that the environment experienced by perylene is increasingly like that of a partially ordered alkane.

The convergence of the perylene environment to that of an alkane as the RTIL alkyl chain length increases is also manifest in the perylene fluorescence spectra displayed in Figure 3. The spectra are normalized at their peaks for clarity. As the RTIL chain length increases, the spectra become closer to that of perylene in the paraffin oil. The spectra are in accord with the trends seen in the friction coefficient data given in Table 3. The fluorescence spectra are sensitive to the local solvent environment and the orientational relaxation data depend on how the environment influences the dynamic interactions between the nonpolar perylene fluorophore and its environment. Both types of data show that as the chain length increases, perylene finds its environment approaching that of a hydrocarbon liquid.

These convergent trends of perylene demonstrate that the solvation environment of perylene in the ionic liquids becomes more alkane-like as the alkyl chain increases in length. In the context of ionic liquid structure, one might conclude that the aliphatic moiety is dominant in solvating the perylene. This is consistent with simulations on solvation in ionic liquids,^{31,32} as well as a recent optical Kerr effect experiment.³³ The selective

**Figure 3.** Normalized fluorescence spectra of perylene in four RTILs and paraffin oil.**Figure 4.** Orientational relaxation times, $\tau = 1/6D$ for MPTS in five solvents plotted as a function of the viscosity (η) divided by kT (symbols). The lines through the data points are fits using linear least-squares. For clarity, the C₂mim⁺ and C₄mim⁺ data have been shifted up 4 and 2 ns, respectively. Because of the difference in time scale, the data for the solvents DMSO and water are shown in the inset. The axes labels for the inset are the same as for the main panel of the figure.

solvation constitutes an effective partitioning of the perylene into the hydrophobic regions of the bulk ionic liquid structure. The subslip rotational behavior is describing the structure and microviscosity of the hydrophobic pockets. It is important to note the apparent lack of a “turn-on” of nanoscale segregation. Both the in-plane and out-of-plane friction coefficients change continuously toward those of perylene in paraffin oil.

This interpretation leads to several interesting possibilities. Although not necessarily of the same origin, void spaces in RTILs have been evoked when discussing the solubility of CO₂.³⁴ The directionality of the rotational friction (see Table 3) may provide insight into anomalous Diels–Alder reactions in RTILs.³⁵ Tiwari and co-workers find that the rate of an intramolecular Diels–Alder reaction involving a nonpolar reactant does not change significantly in going from C₄mim⁺ NTf₂⁻ to C₄mim⁺ [BF₄]⁻, even though the viscosity changes substantially. The reaction involves the rotation of the dienophile over the plane of the molecule. This is the direction of rotation in C₄mim⁺ that is most strongly subslip, indicating a relatively unhindered rotation produced by the ionic liquid structure that should be relatively insensitive to the anion.

B. MPTS. The anisotropy decays of MPTS in all liquids are single exponential, reflecting the lower symmetry of MPTS compared to perylene and indicating similar MPTS rotational diffusion coefficients for the various axes. The decay times vs η/kT are shown in Figure 4 for three RTILs, DMSO, and water. MPTS is essentially insoluble in C₈mim⁺, so this liquid could not be studied. Because of the low viscosity, the data for MPTS in DMSO and water have very fast decay times. The data for these two liquids are shown in the inset. As is the case for perylene, the MPTS temperature dependent data in each liquid is linear within a very small error, demonstrating Debye–Stokes–Einstein behavior.

The friction coefficients for the five liquids are given in Table 4. The friction coefficient for stick boundary conditions is 1. In contrast to the perylene (see Table 2), the MPTS friction coefficients are all greater than 1 for the ionic liquid samples (Table 4), indicating superstick boundary conditions. MPTS in water and DMSO were used as control solvents for comparison. MPTS in these two solvents yield close to stick boundary conditions. Superstick conditions observed in the RTILs are traditionally explained using either the “solventberg” model³⁶ or Nee-Zwanzig dielectric friction³⁷ (eq 7). The former assumes

TABLE 4: MPTS Exp. Friction Coefficients C

solvent	friction coefficient
$C_2\text{mim}^+$	2.22 ± 0.05
$C_4\text{mim}^+$	2.36 ± 0.03
$C_6\text{mim}^+$	2.77 ± 0.04
water	0.99 ± 0.02
DMSO	1.25 ± 0.01

specific solvent–solute interactions anchor solvent molecules of non-negligible size to the solute, effectively increasing the rotator volume. The latter involves the electrostatic torque between a dipole and the reactive field of the surrounding dielectric cavity, as

$$D = \frac{kT}{6\eta V_f C + \zeta_{\text{NZ}}} \quad (7)$$

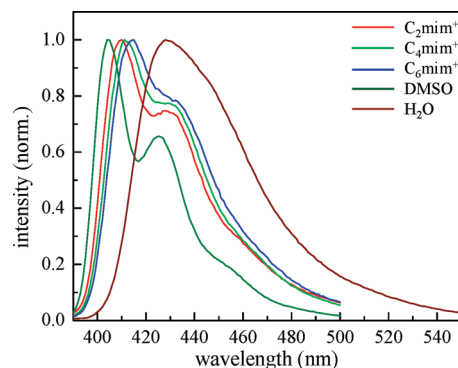
$$\zeta_{\text{NZ}} = \frac{2\mu^2(\epsilon_\infty + 2)^2(\epsilon_0 - \epsilon_\infty)}{a^3 3(2\epsilon_0 + \epsilon_\infty)} \tau_D$$

where μ is the dipole moment of the solute, a is the dielectric cavity radius, τ_D is the Debye relaxation time, and ϵ_0 and ϵ_∞ are the static and optical dielectric constants, respectively.

Given the structure of MPTS, both mechanisms are expected to contribute in the ionic liquid samples. The three formal -1 charged sulfonate groups should interact very strongly with the charged cations of the ionic liquid. Similarly, the presence of a reasonably strong dipole and long Debye relaxation time could also contribute to a dielectric friction. For alcohol solvents that can hydrogen bond to the solute, research on the relative contributions of the two mechanisms has indicated that the “solventberg” effect dominates.³⁸

For the RTILs studied here, the contribution from the dielectric friction was estimated using eq 7 with aggressive but not unrealistic physical parameters and measured properties of the ionic liquids. Taking $\mu = 15$ D,³⁹ $a = 6$ Å,³⁹ $\tau_D = 500$ ps,⁴⁰ $\epsilon_0 = 10$,⁴¹ and $n^2 = \epsilon_\infty = 1.4$,⁴⁰ one arrives at an additional contribution to the friction that is <0.8 . This contribution is in addition to the value of 1, which is the mechanical friction for stick boundary conditions. The actual contribution will most likely be significantly smaller because the RTIL solvents are charged resulting in a reduction caused by the kinetic polarization deficiency and shielding.⁴² With rotational frictions that exceeds stick boundary conditions by greater than a factor of 2 (see Table 4), the dielectric friction alone cannot account for the observed superstick results.

Figure 5 shows the fluorescence spectra of MPTS in the three RTILs and in DMSO and water. MPTS in the three RTILs shows a significant shift to longer wavelengths and a reduction of vibronic structure relative to DMSO. The loss of vibronic structure and bathochromic shift of the fluorescence is indicative of strong solvent–solute interactions.⁴³ The shift and reduction of vibronic structure increases as the alkyl chain length of the RTIL increases. This trend may indicate stronger solute–solvent interactions because of increased segregation of the liquid into ionic regions and alkane-like regions, which is in accord with the trends seen for perylene. The shift in the MPTS spectrum and reduction in vibronic structure with increasing RTIL chain length tracks the observed increase in the friction coefficient (see Table 4). The fluorescence spectrum of MPTS in water shows a very large shift and virtual complete loss of vibronic structure. The spectrum in water indicates that water has a very

**Figure 5.** Normalized fluorescence spectra of MPTS in three RTILs, DMSO, and water.

strong interaction with MPTS. Water is both a hydrogen bond donor and acceptor. Water can solvate the sulfonate anions, and it may also donate π -hydrogen bonds to the aromatic rings. In spite of the spectroscopic evidence for strong interaction between MPTS and water, orientational relaxation occurs with a diffusion constant that is consistent with stick boundary condition. This is in contrast to MPTS in the RTILs that undergoes orientational relaxation that is much slower than stick boundary conditions (see Table 4). Therefore, the strength of the fluorophore–solvent interaction that influences the fluorescence spectrum alone is not sufficient to explain the very slow diffusion, that is, superstick boundary conditions see in Table 4.

The MPTS orientational relaxation data show strongly hindered motion that is likely caused by strongly associated solvent molecules. The most obvious possibility is that RTIL cations are bound to the sulfonate anions. A simple calculation can estimate the number of associated solvent molecules assuming the overall shape factor does not change substantially. Using the cation van der Waals volumes, the results yield 3.0, 2.8, and 3.1 cations that are “attached” to each MPTS in $C_2\text{mim}^+$, $C_4\text{mim}^+$, and $C_6\text{mim}^+$, respectively. These numbers, which are all basically 3, correspond to the number of sulfonate groups on MPTS, supporting the idea that cation coordination is responsible for the slow (superstick) orientational relaxation of MPTS in the RTILs. Furthermore, the friction coefficient increases as the RTIL cation alkyl chain increases. The increase in friction is consistent with larger and larger cations being strongly bound to the MPTS sulfonate groups as RTIL solvent goes from $C_2\text{mim}^+$ to $C_4\text{mim}^+$ to $C_6\text{mim}^+$.

IV. Concluding Remarks

The rotational friction of perylene and MPTS have been studied in a series of 1-alkyl-3-methylimidazolium bis(trifluoromethanesulfonyl)imide ionic liquids from 298 to 333 K. On the basis of these measurements, two distinct rotational environments were found. Perylene undergoes orientational relaxation in the slip to subslip regime, that is orientational relaxation is faster than predicted by hydrodynamic theory. As the alkyl chain length of the cation increases, the in-plane and out-of-plane orientational relaxation friction coefficients converge to those of perylene in paraffin oil (see Table 3). The results indicate that perylene partitions into alkane-like environments. The trends in the in-plane and out-of-plane friction coefficients suggest some degree of alkyl chain alignment along the perylene long molecular axis.

MPTS undergoes orientational relaxation with superstick boundary conditions in contrast to MPTS in DMSO and water, which show approximately stick boundary conditions. The slow

orientational relaxation of MPTS in the RTILs cannot be ascribed to a nonspecific strong solute solvent interaction. The fluorescence spectrum of MPTS in water indicates stronger interactions with water than with the RTILs yet water does not produce anomalously slow orientational relaxation. The results indicate that three RTIL cations are bound to the three MPTS sulfonate anions, and the entire assembly undergoes orientational diffusion. The increased volume of MPTS accounts for the slow orientational diffusion. The friction increases with increasing size of the solvent cation, which is consistent with the picture of cations bound to the MPTS sulfonate anion.

The results presented here provide clear evidence for solutes partitioning into distinct environments in RTILs. The location of the solute depends on its properties, in this case nonionic/nonpolar (perylene) vs highly charged (MPTS) solutes. For both solutes, the orientational dynamics change with the cation alkyl chain length, but for different reasons. As the alkyl chain length increases, perylene finds itself in an increasingly alkane like environment, while MPTS has increasingly large cations bound to it.

Acknowledgment. We would like to thank Professor G. Fuller, Stanford University, for use of his rheometer. This work was supported by the Air Force Office of Scientific Research (F49620-01-1-0018) and the National Science Foundation (DMR 0652232).

References and Notes

- (1) Sureshkumar, M.; Lee, C. K. *J. Mol. Catal. B: Enzym.* **2009**, *60*, 1.
- (2) Paczal, A.; Kotschy, A. *Monatsh. Chem.* **2007**, *138*, 1115.
- (3) Harjani, J. R.; Naik, P. U.; Nara, S. J.; Salunkhe, M. M. *Curr. Org. Synth.* **2007**, *4*, 354.
- (4) Li, Z. J.; Chang, J.; Shan, H. X.; Pan, J. M. *Rev. Anal. Chem.* **2007**, *26*, 109.
- (5) Hagiwara, R.; Lee, J. S. *Electrochemistry* **2007**, *75*, 23.
- (6) Canongia Lopes, J.; Padua, A. A. H. *J. Phys. Chem. B* **2006**, *110*, 3330.
- (7) Triolo, A.; Russina, O.; Bleif, H. J.; Di Cola, E. *J. Phys. Chem. B* **2007**, *111*, 4641.
- (8) Iwata, K.; Okajima, H.; Saha, S.; Hamaguchi, H. *Acc. Chem. Res.* **2007**, *40*, 1174.
- (9) Xiao, D.; Rajian, J. R.; Hines, L. G.; Li, S.; Bartsch, R. A.; Quitevis, E. L. *J. Phys. Chem. B* **2008**, *112*, 13316.
- (10) Shiget, S.; Hamaguchi, H. *Chem. Phys. Lett.* **2006**, *427*, 329.
- (11) Hu, Z. H.; Margulis, C. J. *Proc. Natl. Acad. Sci. U.S.A.* **2006**, *103*, 831.
- (12) Jin, H.; Li, X.; Maroncelli, M. *J. Phys. Chem. B* **2007**, *111*, 13473.
- (13) Davis, J. H. *Chem. Lett.* **2004**, *33*, 1072.
- (14) Ingram, J. A.; Moog, R. S.; Ito, N.; Biswas, R.; Maroncelli, M. *J. Phys. Chem. B* **2003**, *107*, 5926.
- (15) Mali, K. S.; Dutt, G. B.; Mukherjee, T. J. *Chem. Phys.* **2008**, *128*, 054504.
- (16) Ito, N.; Arzhantsev, S.; Maroncelli, M. *Chem. Phys. Lett.* **2004**, *396*, 83.
- (17) Funston, A. M.; Fadeeva, T. A.; Wishart, J. F.; Castner, E. W. *J. Phys. Chem. B* **2007**, *111*, 4963.
- (18) Spry, D. B.; Goun, A.; Glusac, K.; Moilanen, D. E.; Fayer, M. D. *J. Am. Chem. Soc.* **2007**, *129*, 8122.
- (19) Tokuda, H.; Hayamizu, K.; Ishii, K.; Susan, M. A. B. H.; Watanabe, M. *J. Phys. Chem. B* **2005**, *109*, 6103.
- (20) Chuang, T. J.; Eiselthal, K. B. *J. Chem. Phys.* **1972**, *57*, 5094.
- (21) Perrin, F. *J. Phys. Radium* **1936**, *7*, 1.
- (22) Sension, R. J.; Hochstrasser, R. M. *J. Chem. Phys.* **1993**, *98*, 2490.
- (23) Youngren, G. K.; Acrivos, A. *J. Chem. Phys.* **1975**, *63*, 3846.
- (24) Xu, J.; Shen, X.; Knutson, J. R. *J. Phys. Chem. A* **2003**, *107*, 8383.
- (25) Kim, Y. R.; Hochstrasser, R. M. *J. Phys. Chem.* **1992**, *96*, 9595.
- (26) Mannekutla, J. R.; Ramamurthy, P.; Mulimani, B. G.; Inamdar, S. R. *J. Chem. Phys.* **2007**, *340*, 149.
- (27) Wirth, M. J.; Chou, S. H. *J. Phys. Chem.* **1991**, *95*, 1786.
- (28) Pauls, S. W.; Hedstrom, J. F.; Johnson, C. K. *J. Chem. Phys.* **1998**, *237*, 205.
- (29) Jiang, Y.; Blanchard, G. J. *J. Phys. Chem.* **1994**, *98*, 6436.
- (30) Troxler, T.; Stratton, J. R.; Smith, P. G.; Topp, M. R. *J. Chem. Phys.* **1994**, *101*, 9219.
- (31) Chaumont, A.; Wipff, G. *J. Mol. Liq.* **2007**, *131*, 36.
- (32) Padua, A. A. H.; Gomes, M. F.; Lopes, J. N. A. C. *Acc. Chem. Res.* **2007**, *40*, 1087.
- (33) Xiao, D.; Hines, L. G.; Bartsch, R. A.; Quitevis, E. L. *J. Phys. Chem. B* **2009**, *113*, 4544.
- (34) Blanchard, L. A.; Gu, Z.; Brennecke, J. F. *J. Phys. Chem. B* **2001**, *105*, 2437.
- (35) Tiwari, S.; Khupse, N.; Kumar, A. *J. Org. Chem.* **2008**, *73*, 9075.
- (36) Spears, K. G.; Cramer, L. E. *J. Chem. Phys.* **1978**, *30*, 1.
- (37) Nee, T.-W.; Zwanzig, R. *J. Chem. Phys.* **1970**, *52*, 6353.
- (38) Horng, M.-L.; Gardecki, J. A.; Maroncelli, M. *J. Phys. Chem. A* **1997**, *101*, 1030.
- (39) Balabai, N.; Sukharevsky, A.; Read, I.; Strazisar, B.; Kurnikova, M.; Hartman, R. S.; Coalson, R. D.; Waldeck, D. H. *J. Mol. Liq.* **1998**, *77*, 37.
- (40) Daguene, C.; Dyson, P. J.; Krossing, I.; Oleinikova, A.; Slattery, J.; Wakai, C.; Weingartner, H. *J. Phys. Chem. B* **2006**, *110*, 12682.
- (41) Weingartner, H. *Z. Phys. Chem.* **2006**, *220*, 1395.
- (42) Hubbard, J. B.; Onsager, L.; van Beek, W. M.; Mandel, M. *Proc. Natl. Acad. Sci. U.S.A.* **1977**, *74*, 401.
- (43) Lakowicz, J. R. *Principles of Fluorescence Spectroscopy*, 3rd ed.; Springer: New York, 2006.

JP911123V